Electronic Supplementary Information

High-Efficiency Non-Fullerene Organic Solar Cells Enabled by a Difluorobenzothiadizole-Based Donor Polymer Combined with a Properly Matched Small Molecule Acceptor

Jingbo Zhao,[a,§] Yunke Li,[a,§] Haoran Lin,[a,§] Yuhang Liu,[a,c] Kui Jiang, [a,b] Cheng Mu,[a] Tingxuan Ma,[a,c] Joshua Yuk Lin Lai,[a] Huawei Hu,[a,c] Demei Yu[c] and He Yan[a,b,*]

[a] Department of Chemistry, The Hong Kong University of Science and Technology, Clear Water Bay, Hong Kong.
[b] HKUST-Shenzhen Research Institute, No. 9 Yuexing 1st RD, Hi-tech Park, Nanshan, Shenzhen 518057, China.
[c] Joint School of Sustainable Development and MOE Key Lab for Non-Equilibrium Synthesis and Modulation of Condensed Matter., Xi'an Jiaotong University, Xi'an 710049, P R China.
[§] These authors contributed equally.
Email: hyan@ust.hk

I. Materials and Methods:

Materials. All reagents and chemicals were purchased from commercial sources and used without further purification unless stated otherwise. PTB7-Th was purchased from 1-Material. SF-PDI$_2$ [1] and di-PDI [2] were synthesized according to literature procedure and further purified by recrystallization from $CHCl_3$/MeOH. PffBT4T-2DT was synthesized using modified literature procedure.[3]

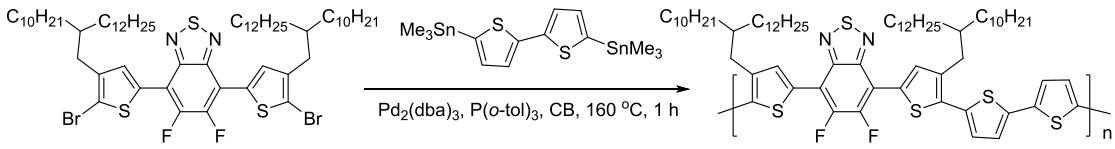

S1 **PffBT4T-2DT**

PffBT4T-2DT. The polymer was synthesized by microwave assisted reaction. To a microwave tube was added monomer **S1** (100 mg, 0.086 mmol), 5,5'-bis(trimethylstannyl)-2,2'-bithiophene (42.3 mg, 0.086 mmol), $Pd_2(dba)_3$ (1.1 mg, 0.002 mmol), P(*o*-tol)$_3$ (2.4 mg, 0.008 mmol) and 1.6 mL of anhydrous chlorobenzene in a glove box protected with N_2. The microwave tube was then sealed and heated at 160 ℃ for 1 hour in a microwave reactor. The mixture was cooled to room temperature and 10 mL toluene was added before precipitated from methanol. The solid was collected by filtration, and loaded into an extraction thimble and washed successively with acetone and dichloromethane. The polymer was finally collected from chloroform. The chloroform solution was then concentrated and precipitated into methanol. The solid was collected by filtration and dried in vacuo to get the polymer as dark green solid (53 mg, 54%).

AFM analysis. AFM measurements were performed by using a Scanning Probe Microscope-Dimension 3100 in tapping mode. All film samples were spincasted on ITO/ZnO substrates.

Optical characterizations. UV-Vis absorption spectra were acquired on a Perkin Elmer Lambda 20 UV/VIS Spectrophotometer. All film samples were spincast on ITO/ZnO substrates. PL spectra were measured on samples on ITO/ZnO substrates upon excitation of a laser beam using a Renishaw RM 3000 Micro-Raman/Photoluminescence system. All film samples were spincasted on ITO/ZnO substrates.

Electrochemical characterizations. Cyclic voltammetry was carried out on a CHI760E electrochemical workstation with three electrodes configuration, using Ag/AgCl as the reference electrode, a Pt plate as the counter electrode, and a glassy carbon as the working electrode. Polymers were drop-cast onto the electrode from chlorobenzene solutions (2 g L^{-1}) to form thin films. 0.1 mol L^{-1} tetrabutylammonium

hexafluorophosphate in anhydrous acetonitrile was used as the supporting electrolyte. Small molecule samples were tested in dichloromethane solution (1.0×10^{-4} mol L^{-1}) with the same supporting electrolyte. Potentials were referenced to the ferrocenium/ferrocene couple by using ferrocene as external standards in dichloromethane or acetonitrile solutions. The scan rate is 0.1 V s^{-1}. The solution was degassed by bubbling nitrogen for 20 minutes before measurement.

Hole mobility measurements. The hole mobilities were measured using the space charge limited current (SCLC) method, employing a device architecture of ITO/V_2O_5/blend film/V_2O_5/Al. The mobilities were obtained by taking current-voltage curves and fitting the results to a space charge limited form, where the SCLC is described by:

$$J = \frac{9\varepsilon_0\varepsilon_r\mu(V_{appl} - V_{bi} - V_s)^2}{8L^3}$$

Where ε_0 is the permittivity of free space, ε_r is the relative permittivity of the material (assumed to be 3), μ is the hole mobility, V_{appl} is the applied voltage, V_{bi} is the built-in voltage (0 V)[4], V_s is the voltage drop from the substrate's series resistance ($V_s = IR$, R is measured to be 10.8 Ω) and L is the thickness of the film. The J~V_{appl} and $J^{1/2}$~(V_{appl}-V_{bi}-V_s) characteristics are shown in Fig. S2. By linearly fitting $J^{1/2}$ with V_{appl}-V_{bi}-V_s, the mobilities were extracted from the slope and L:

$$\mu = \frac{\text{slope}^2 \times 8L^3}{9\varepsilon_0\varepsilon_r}$$

Electron mobility measurements. The electron mobilities were measured using the SCLC method, employing a device architecture of ITO/ZnO/blend film/Ca/Al. The mobilities were obtained by taking current-voltage curves and fitting the results to a space charge limited form, where the SCLC is described by:

$$J = \frac{9\varepsilon_0\varepsilon_r\mu(V_{appl} - V_{bi} - V_s)^2}{8L^3}$$

Where ε_0 is the permittivity of free space, ε_r is the relative permittivity of the material (assumed to be 3), μ is the electron mobility, V_{appl} is the applied voltage, V_{bi} is the built-in voltage (0.7 V)[4], V_s is the voltage drop from the substrate's series resistance ($V_s = IR$, R is measured to be 10.8 Ω) and L is the thickness of the film. The J~V_{appl} and $J^{1/2}$~(V_{appl}-V_{bi}-V_s) characteristics are shown in Fig. S3. By linearly fitting $J^{1/2}$ with V_{appl}-V_{bi}-V_s, the mobilities were extracted from the slope and L:

$$\mu = \frac{\text{slope}^2 \times 8L^3}{9\varepsilon_0\varepsilon_r}$$

Calculation of charge dissociation probabilities, *P*(*E*,*T*). $P(E,T)$ at short circuit is calculated following commonly used procedure.[5-9]

$$P(E,T) = \frac{J_{ph}(\text{SC})}{J_{ph}(\text{saturated})}$$

Where J_{ph}(SC) is the photocurrent at short circuit, J_{ph}(saturated) is the saturated photocurrent at reversed bias. Here J_{ph}(saturated) is assumed to be equal to J_{ph} at a voltage of -6 V, because J_{ph} becomes independent of the applied voltage at around -6 V. The results are listed in Table S1.

Solar cell fabrication and testing. Pre-patterned ITO-coated glass with a sheet resistance of ~15 Ω per square was used as the substrate. It was cleaned by sequential sonications in soap deionized water, deionized water, acetone, and isopropanol for 15 min at each step. After UV/ozone treatment for 60 min, a ZnO electron transport layer was prepared by spin-coating at 5000 rpm from a ZnO precursor solution (diethyl zinc). Active layer solutions (D/A ratio 1:1.4) were prepared in CB (polymer concentration: 6.5 mg/mL). To completely dissolve the polymer, the active layer solution should be stirred on hotplate at 110 ℃ for at least 3 hours. Before spincoating, both the polymer solution and ITO substrate are preheated on a hotplate at about 110 ℃. Active layers were spin-coated from the warm polymer solution on the preheated substrate in a N_2 glovebox at 1200 rpm to obtain thicknesses of ~120 nm. The polymer:SMA blend films were then annealed at 100 ℃ for 5 min before being transferred to the vacuum chamber of a thermal evaporator inside the same glovebox. At a vacuum level of 3×10^{-6} Torr, a thin layer (20 nm) of V_2O_5 was deposited as the anode interlayer, followed by deposition of 100 nm of Al as the top electrode. All cells were encapsulated using epoxy inside the glovebox. Device *J-V* characteristics was measured under AM1.5G (100 mW cm^{-2}) using a Newport solar simulator. The light intensity was calibrated using a standard Si diode (with KG5 filter, purchased from PV Measurement) to bring spectral mismatch to unity. *J-V* characteristics were recorded using a Keithley 236 source meter unit. Typical cells have devices area of 5.9 mm^2, which is defined by a metal mask with an aperture aligned with the device area. EQEs were characterized using a Newport EQE system equipped with a standard Si diode. Monochromatic light was generated from a Newport 300W lamp source.

II. Supplementary figures and tables.

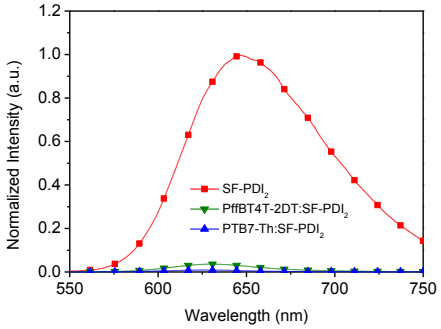

Fig. S1 PL quenching spectra of SF-PDI_2, PffBT4T-2DT:SF-PDI_2 blend and PTB7-Th:SF-PDI_2 blend. Excitation of the films was at 514 nm. Each spectrum was corrected for the absorption of the film at the excitation wavelength.

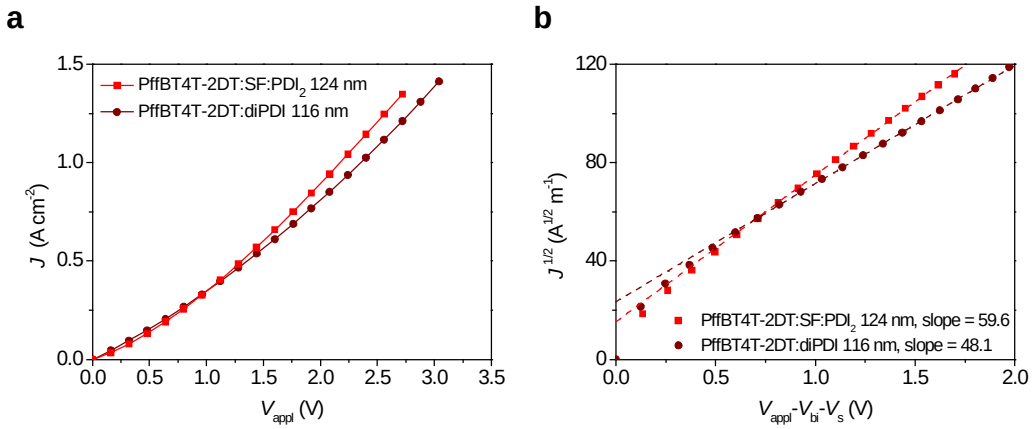

Fig. S2 (a) J~V_{appl} and (b) $J^{1/2}$~(V_{appl}-V_{bi}-V_s) characteristics of hole only devices. Dash lines are fits.

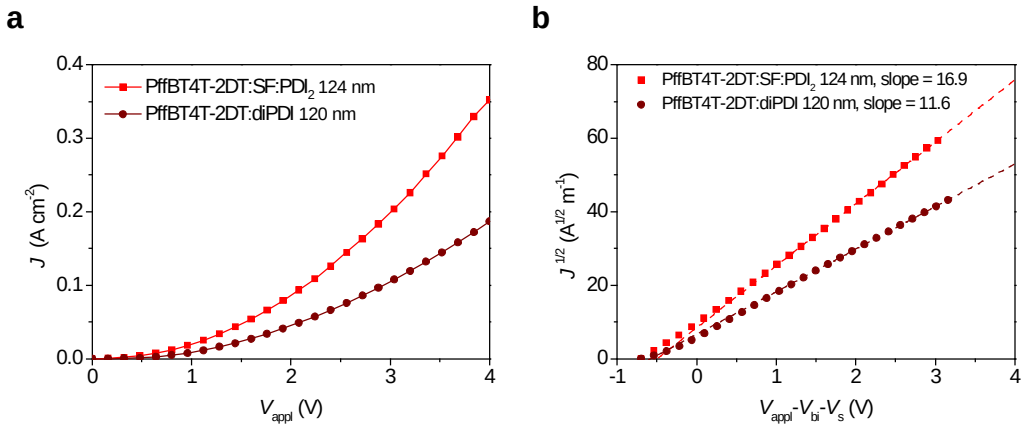

Fig. S3 (a) J~V_{appl} and (b) $J^{1/2}$~(V_{appl}-V_{bi}-V_s) characteristics of electron only devices. Dash lines are fits.

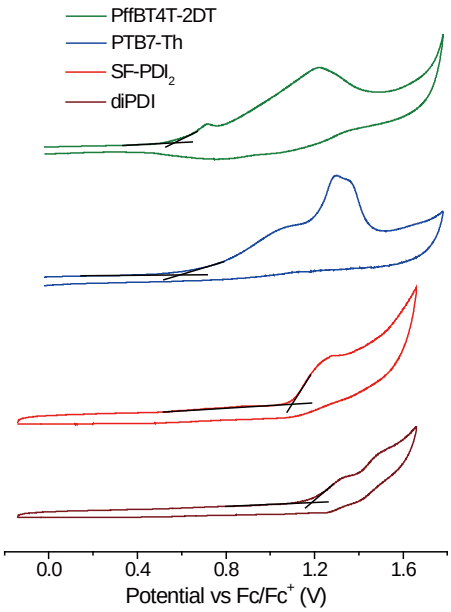

Fig. S4 Cyclic voltammograms of PffBT4T-2DT, PTB7-Th, SF-PDI_2 and diPDI.

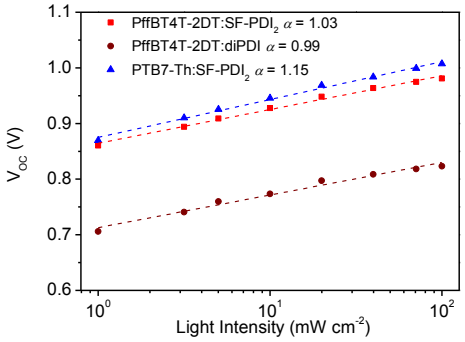

Fig. S5 Light intensity dependence of the open circuit voltage of the devices. Dash lines are fits (V_{OC} = $\alpha k_B T/q$ ln P + constant). The calculated α values of the devices are shown in the figure, which indicate the stronger monomolecular (Shockley-Read-Hall) recombination at open circuit in the device of PTB7-Th:SF-PDI_2.

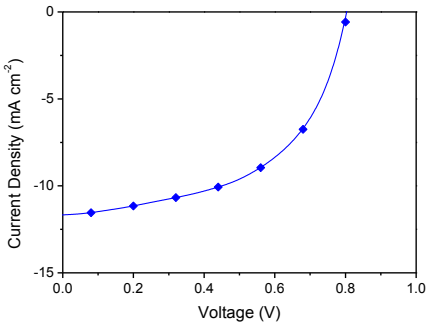

Fig. S6 *J-V* characteristics of an unoptimized PTB7-Th:diPDI device without using interlayers showing a V_{OC} = 0.805 V, J_{SC} = 11.67 mA cm^{-2}, FF = 0.535 and PCE = 5.03%, which is comparable with the literature report.[10]

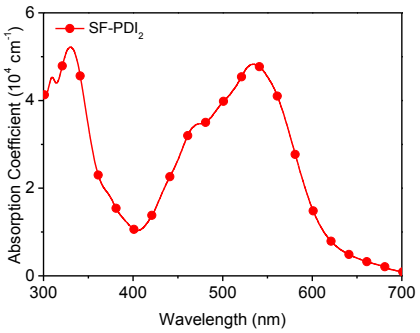

Fig. S7 Film absorption co-efficients of SF-PDI_2.

Table S1 Calculation of $P(E,T)$ of the three photovoltaic devices

Active layer	J_{ph}(SC)	J_{ph}(saturated)	$P(E,T)$
PffBT4T-2DT:SF-PDI_2	10.7	13.6	79%
PffBT4T-2DT:diPDI	12.2	15.1	81%
PTB7-Th:SF-PDI_2	7.4	15.0	49%

Table S2 The detailed photovoltaic performances of the solar cells based on PffBT4T-2DT:SF-PDI_2 with different donor:acceptor ratios.

D:A ratio	V_{OC} [V]	J_{SC} [mA cm^{-2}]	FF	PCE [%]
1:1	0.97	9.9	0.57	5.4
1:1.4	0.99	11.0	0.58	6.3
1:1.8	0.96	10.4	0.56	5.6
1:2.5	0.97	8.1	0.43	3.4

References

1. Q. F. Yan, Y. Zhou, Y. Q. Zheng, J. Pei and D. H. Zhao, *Chem. Sci.*, 2013, **4**, 4389-4394.
2. W. Jiang, L. Ye, X. G. Li, C. Y. Xiao, F. Tan, W. C. Zhao, J. H. Hou and Z. H. Wang, *Chem. Commun.*, 2014, **50**, 1024-1026.
3. Z. Chen, P. Cai, J. Chen, X. Liu, L. Zhang, L. Lan, J. Peng, Y. Ma and Y. Cao, *Adv. Mater.*, 2014, **26**, 2586-2591.
4. X. G. Guo, N. J. Zhou, S. J. Lou, J. Smith, D. B. Tice, J. W. Hennek, R. P. Ortiz, J. T. L. Navarrete, S. Y. Li, J. Strzalka, L. X. Chen, R. P. H. Chang, A. Facchetti and T. J. Marks, *Nat. Photon.*, 2013, **7**, 825-833.
5. L. Lu, T. Xu, W. Chen, E. S. Landry and L. Yu, *Nat. Photon.*, 2014, **8**, 716-722.
6. S. R. Cowan, A. Roy and A. J. Heeger, *Phys. Rev. B*, 2010, **82**, 245207.
7. V. D. Mihailetchi, L. J. A. Koster, P. W. M. Blom, C. Melzer, B. de Boer, J. K. J. van Duren and R. A. J. Janssen, *Adv. Funct. Mater.*, 2005, **15**, 795-801.
8. Z. Li, J. D. A. Lin, H. Phan, A. Sharenko, C. M. Proctor, P. Zalar, Z. Chen, A. Facchetti and T.-Q. Nguyen, *Adv. Funct. Mater.*, 2014, DOI: 10.1002/adfm.201401367.

9. L. Ye, W. Jiang, W. Zhao, S. Zhang, D. Qian, Z. Wang and J. Hou, *Small*, 2014, DOI: 10.1002/smll.201401082.
10. Y. Zang, C. Z. Li, C. C. Chueh, S. T. Williams, W. Jiang, Z. H. Wang, J. S. Yu and A. K. Jen, *Adv. Mater*., 2014, **26**, 5708-5714.